Tandem Hydroformylation-Aldol Condensation Reaction Enabled by Zn-MOF-74

Journal Article

Author(s):
Gäumann, Patrick; Rohrbach, Thomas; Artiglia, Luca; Ongari, Daniele; Smit, Berend; van Bokhoven, Jeroen A.; Ranocchiari, Marco

Chemistry–A European Journal

Research Article
doi.org/10.1002/chem.202300939

Chemistry Europe
European Chemical
Societies Publishing

www.chemeurj.org

Tandem Hydroformylation-Aldol Condensation Reaction Enabled by Zn-MOF-74

Patrick Gäumann,[a] Thomas Rohrbach,[a] Luca Artiglia,[a] Daniele Ongari,[b] Berend Smit,[b] Jeroen A. van Bokhoven,[a, c] and Marco Ranocchiari*[a, d]

Abstract: The tandem hydroformylation-aldol condensation (tandem HF-AC) reaction offers an efficient synthetic route to the synthesis of industrially relevant products. The addition of Zn-MOF-74 to the cobalt-catalyzed hydroformylation of 1-hexene enables tandem HF-AC under milder pressure and temperature conditions than the aldox process, where zinc salts are added to cobalt-catalyzed hydroformylation reactions to promote aldol condensation. The yield of the aldol condensation products increases by up to 17 times compared to that of the homogeneous reaction without MOF and up to 5 times compared to the aldox catalytic system. Both $Co_2(CO)_8$ and Zn-MOF-74 are required to significantly enhance the activity of the catalytic system. Density functional theory simulations and Fourier-transform infrared experiments show that heptanal, the product of hydroformylation, adsorbs on the open metal site (OMS) of Zn-MOF-74, thereby increasing the electrophilic character of the carbonyl carbon atom and facilitating the condensation.

Introduction

Metal–organic frameworks (MOFs) consist of organic linkers connected to metal ions or clusters.[1] They are crystalline and are among the materials with the highest surface areas.[2] MOFs are modularly built and allow for modifications in the linker and the metal node. This variety leads to a wide collection of possible structures that are tunable for targeted properties and enable application in catalysis,[3] gas storage,[4] and gas separation.[5] Hydroformylation (HF) is one of the most important processes using homogeneous catalysts and includes the addition of molecular hydrogen and carbon monoxide to a

carbon-carbon double bond to yield aldehydes. This reaction is catalyzed by rhodium and cobalt complexes.[6] Aldehydes are valuable chemicals because they offer synthetic pathways to alcohols, amines, carboxylic acids, esters, and other functionalized molecules.[6] Various reports highlight the use of MOFs in HF reactions.[7] MOFs influence the distribution between *linear* and *iso* aldehydes in HF. Our group showed that the addition of Zn-MOF-74 to the cobalt-catalyzed HF of linear aliphatic alpha olefins yields the branched aldehydes with up to 90% selectivity compared to the 50% selectivity in the system without MOF. The reason for this high selectivity is attributed to the more efficient packing of the olefin molecules inside the MOF pores, which leads to a higher alkene concentration favoring the kinetics of formation of the branched product.[7a] MOFs find application in HF for the heterogenization of the catalyst to facilitate its recycling and separation. Hou et al. immobilized rhodium nanoparticles on ZIF-8 and used this catalyst (Rh@ZIF-8) in the HF of linear olefins with various chain lengths and styrene. The catalyst was recycled five times without significant loss of activity.[7b] Sartipi et al. synthesized a phosphotungstic acid (PTA)-containing derivative of MIL-101(Cr) (PTA-MIL-101(Cr)). This composite was used in a catch-and-release system with $RhH(CO)(PPh_3)_3$. Under ambient atmosphere, rhodium coordinates to PTA, whereas under reaction conditions, CO coordinates to the metal leading to a homogeneous catalyst. After the reaction, the catalyst recoordinates to PTA-MIL-101(Cr) upon the release of syngas pressure. This system allowed the successful recycling of the catalyst in six consecutive runs without loss in HF activity.[7c] Tang et al. synthesized a MOF with dipyrazole linkers and metalated it with cobalt and rhodium species. The rhodium catalyst showed full conversion in the HF of styrene in three consecutive runs.[7d]

Aldol condensation (AC) is a reaction between an enolizable aldehyde or ketone and a nucleophilic carbonyl compound to form β-hydroxy aldehydes (aldols) and β-hydroxy ketones

[a] P. Gäumann, T. Rohrbach, Dr. L. Artiglia, Prof. Dr. J. A. van Bokhoven, Dr. M. Ranocchiari
Laboratory for Catalysis and Sustainable Chemistry
Paul Scherrer Institut
Forschungsstrasse 111, 5232 Villigen PSI (Switzerland)
E-mail: marco.ranocchiari@psi.ch
Homepage: http://www.psi.ch/en/syncat

[b] Dr. D. Ongari, Prof. Dr. B. Smit
Laboratory of Molecular Simulation (LSMO)
Institut des Sciences et Ingénierie Chimiques, Valais
Ecole Polytechnique Fédérale de Lausanne (EPFL)
Rue de l' Industrie 17, 1951 Sion (Switzerland)

[c] Prof. Dr. J. A. van Bokhoven
Institute for Chemical and Bioengineering
Eidgenössische Technische Hochschule (ETH) Zurich
Vladimir-Prelog-Weg 1, 8093 Zurich (Switzerland)

[d] Dr. M. Ranocchiari
Energy System Integration
Paul Scherrer Institut
Forschungsstrasse 111, 5232 Villigen PSI (Switzerland)

Chem. Eur. J. **2023**, *29*, e202300939 (1 of 7)

© 2023 The Authors. Chemistry - A European Journal published by Wiley-VCH GmbH

Chemistry–A European Journal | Research Article
doi.org/10.1002/chem.202300939

Chemistry
Europe
European Chemical
Societies Publishing

(ketols). In the condensation step, α,β-unsaturated aldehydes or ketones form upon release of one equivalent water.[8] It is a powerful tool used by organic chemists for the formation of C—C bonds.[9] This reaction is acid- and, more frequently, base-catalyzed.[8b] AC is a known side reaction in HF[10] and is generally more pronounced in cobalt-catalyzed systems compared to those based on rhodium.[11] Such a side reaction may be desirable for the synthesis of more complex molecules.[6] A typical example is the synthesis of 2-ethylhexanol (2-EH), the precursor of the most widely used plasticizer, bis(2-ethylhexyl) phthalate (DEHP),[12] from propene.[13] In a first step, n-butyraldehyde is formed by HF, followed by AC and hydrogenation (hyd.) to yield the desired product (see Scheme 1).

A tandem HF-AC reaction would be beneficial in order to produce aliphatic aldehydes and alcohols; Exxon has been applying the aldox process for their synthesis.[14] Organic zinc salts such as zinc acetylacetonate were added to the reaction mixture to catalyze the AC at 200 atm and 180 °C.[15] The products are hydrogenated in an additional step. A similar system was introduced by Shell, which expanded the standard HF system, tributylphosphane, cobalt carbonyl, with KOH or amines to catalyze the AC.[16] Such processes have been discontinued due to low selectivity and the harsh conditions, under which they take place.

Today fundamental research focuses on tandem HF-AC under milder conditions using for the most part rhodium-based catalysts for the HF and various cocatalysts, such as pyrrolidinium benzoate,[17] aniline,[18] the solid base hydrotalcite,[19] and sodium hydroxide, in a multiphasic system.[20] Catalysts based on platinum and *para*-toluenesulfonic acid[21] have also been studied. A general characteristic of these systems is the high price of the metal and the addition of a second catalyst (acid or base) to promote the AC reaction. A cobalt-based system would be a much cheaper alternative with relatively high hydroformylation activity. While investigating the role of Zn-MOF-74 in the branched-selective, cobalt-catalyzed HF of 1-hexene,[7a] we discovered its enhancing effect on the tandem HF-AC

reaction. Based on this observation, we decided to study its potential in the reaction to target the AC product. Here we will show that Zn-MOF-74 catalyzes the cobalt-based tandem HF-AC, to attain a performance comparable to that of the aldox system under mild conditions by adsorbing the aldehydes that form during HF, thereby enhancing their electrophilicity.

Results and Discussion

Figure 1 shows the product composition as a function of time in the cobalt-catalyzed hydroformylation of 1-hexene at 25 bar syngas pressure and 100 °C.[7a] Under these conditions, tandem HF-AC is a side reaction with the majority of products being 2-ethylpentanal, 2-methylhexanal, heptanal (**2**) and hexene isomers, while the hydrogenation of alkenes was not observed (Table S2). After 8 h, the yield of **3** was 0.18% in the homogeneous reaction (triangles) and 2.1% in the presence of Zn-MOF-74 (squares), i.e., 11 times higher. After 24 h, the yields were 1.2% and 3.9%, respectively, three times higher with the MOF. The addition of Zn-MOF-74 favors not only branched selectivity, but also the yield of the AC product.

To understand the role of the cobalt catalyst and of the MOF in the AC reaction, we studied the reaction of **2** at 25 bar syngas pressure and 100 °C in n-hexane (0.7 M) with all four possible combinations: absence or presences of Zn-MOF-74 and the cobalt catalyst as part of the reaction mixture. Figure 2 shows that the yield of **3** is 1.3% in the absence of both cobalt and MOF. The cobalt catalyst yielded 10%, Zn-MOF-74 6.1%, of **3**. The presence of both the catalyst and MOF yielded **3** in 47%, five and eight times higher than that obtained with the cobalt catalyst and MOF, respectively.

This result led us to perform a series of catalytic experiments focusing on the AC with and without Zn-MOF-74, using a setup
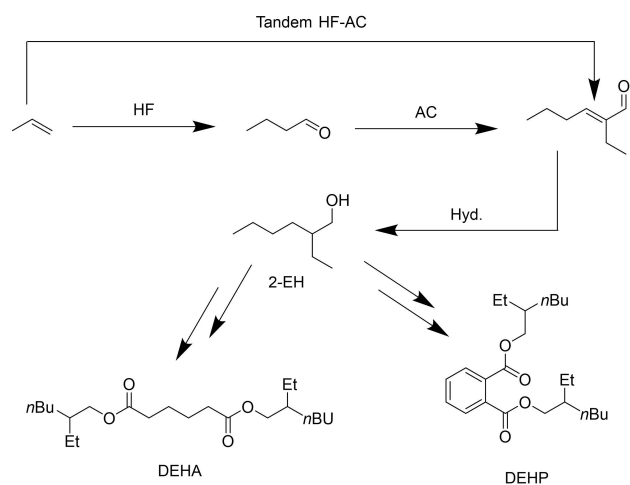
Scheme 1. Industrially relevant products involving hydroformylation followed by aldol condensation reactions in the synthetic pathway.
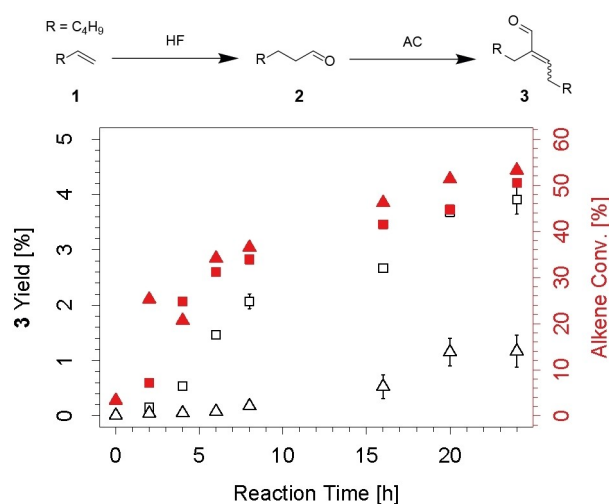
Figure 1. Conversion (red) and corresponding tandem HF-AC **3** yields (black symbols) of the homogeneous hydroformylation of 1-hexene (0.5 mL, 4.0 mmol), catalyzed by $Co_2(CO)_8$ (1.6 mg, 4.7 μmol, triangles) and the Zn-MOF-74-modified (Zn-MOF-74: 20 mg, 43 μmol, $Co_2(CO)_8$: 1.6 mg, 4.7 μmol, squares) reaction as a function of time. The reactions were performed at 25 bar syngas pressure (CO: $H_2 = 1$) and 100 °C.

Chemistry–A European Journal

Research Article
doi.org/10.1002/chem.202300939

Chemistry Europe
European Chemical
Societies Publishing

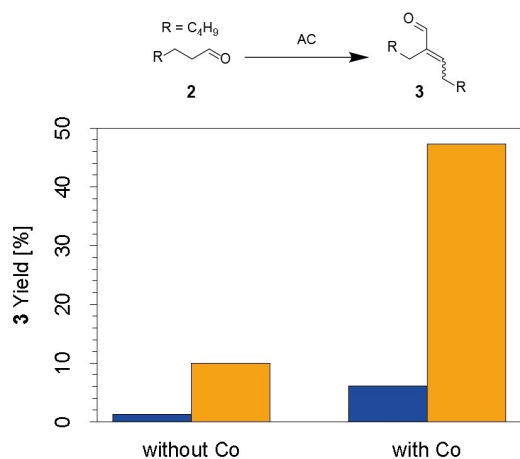**Figure 2.** AC yield of **3** in the four reactions in the absence or presence of $Co_2(CO)_8$ (1.6 mg, 4.7 μmol) and Zn-MOF-74 (20 mg, 43 μmol) using a solution of heptanal in hexane (0.7 M, 0.5 mL, 0.35 mmol) at 25 bar syngas pressure (CO: $H_2 = 1$) and 100 °C, 5 h. Blue and orange bars correspond to reactions without and with Zn-MOF-74, respectively. The experiments (left group) were performed without the cobalt catalyst, while it was added in the other experiments (right group).

allowing for sampling every 15 min to assess the evolution of **3** as a function of time. The results are plotted in Figure 3. All four reactions feature an induction period of 30 min, attributed to the formation of the active species from $Co_2(CO)_8$, the precatalyst of hydroformylation.[22] After the induction period, the profiles of the four reactions are very different. The homogeneous reactions yielded **3** in 12% and 4% after about 5 h at 25 bar (Figure 3, black squares) and at 75 bar syngas pressure (Figure 3, black triangles), respectively. The reactions in the presence of a cobalt catalyst and Zn-MOF-74 showed 29% and 62% yield of **3** after 6 h at 25 bar (Figure 3, red squares) and at 75 bar (Figure 3, red triangles), respectively, a significant
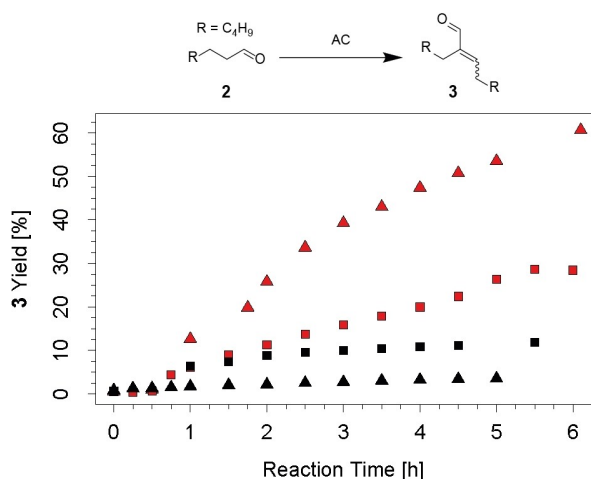

Figure 3. Yield of AC product **3** from heptanal (2.8 M in cyclohexane) as a function of time. The homogenous reaction (black, $Co_2(CO)_8$ (3.2 mg/ml, 9.4 mM) and the MOF-modified reaction (red, $Co_2(CO)_8$ (3.2 mg/ml, 9.4 mM), Zn-MOF-74 (40 mg/ml, 86 μmol/g)) were performed at two pressures 25 bar (squares) and 75 bars (triangles) of syngas (CO: $H_2 = 1$) at 100 °C.

increase of up to 16 times compared to that in the corresponding homogeneous reaction. These trends are noteworthy. While the yield in the homogeneous reaction decreases at higher pressure, that in the presence of the MOF increases. The decrease of AC products at higher pressures is in agreement with the literature.[23] The inversion of this tendency by Zn-MOF-74 confirms its role as promoter in the tandem reaction. Inductively coupled plasma optical emission spectroscopy (ICP-OES) indicated that the majority of the cobalt is adsorbed within the pores of the MOF after 2 h reaction at 25 bar (Figure S7). Up to 2 h, the homogeneous and the MOF-modified reactions follow a similar path because the reactivity of cobalt is dictated by the homogeneous species, which is more than 80% up to 1 h reaction (Figure 3, squares). From 2 h reaction time, the reaction with MOF yielded significantly higher amounts of **3**. This indicates that the cobalt adsorption within the MOF drives the higher AC yield. Experiments in the absence, respectively, in the presence of the cobalt catalyst and MOF were performed at 75 bar syngas pressure and showed the formation of the hydrogenated AC product **4**. The yield of the AC products (**3** and **4**) is 8% with the cobalt catalyst but without the MOF. The addition of Zn-MOF-74 increased the yield to 87%, i.e., by more than a factor of 10 (see Figure S8). The data in Figures 2, 3, and S8 clearly indicate that both cobalt catalyst and MOF are required for the efficient promotion of the AC reaction.

We tested the tandem HF-AC of 1-hexene at 80 bar as a function of temperature. A branched selectivity increase in the hydroformylation reaction was observed in agreement with our previous study[7a] (Tables S3 and S4, Entries 2 and 3). The results in Figure 4 highlight the dramatic effect of temperature on the yield of AC products. At 60 °C, 1-hexene did not react to heptanal, indicating that the AC also did not take place. Temperatures above 110 °C were required to convert more than 90% 1-hexene in the Zn-MOF-74-modified reaction. Conversion of 1-hexene was generally higher in the homogeneous reaction, reaching around 99% at temperatures above 90 °C. High temperatures clearly favor the hyd. of **3** to the saturated aldehyde **4** (Figure 4). While the homogeneous reaction yielded 1.3 and 1.9% AC products at temperatures of 90 °C and 150 °C, respectively, Zn-MOF-74 enhanced the yield of the AC products to 9.0 and 33% (a factor of 6.9 and 17), respectively. At 150 °C, the selectivity to AC products is comparable to the aldox process, while employing much milder conditions.[15] Additional products included 2-ethylpentanal, 2-methylhexanal, heptanal, the corresponding alcohols and heavier products, while no alkanes were observed (Tables S3 and S4). The filtered and washed MOF was used for a second catalytic cycle, giving a 21% and 5.7% yield of **3** and of **4**, respectively, at 110 °C, in good agreement with the pristine MOF (Figure S9). A different zinc source was tested as an additive to verify that the MOF structure was essential to maximize the yield in the tandem HF-AC reaction. The addition of an equimolar amount of zinc as zinc acetylacetonate, as in the aldox reaction, led to a yield of 3.3% of **3** and of 1.6% of **4**. In comparison, the reaction with Zn-MOF-74 afforded the products (20% and 5.7%, respectively) under identical conditions (80 bar syngas, 110 °C). These results
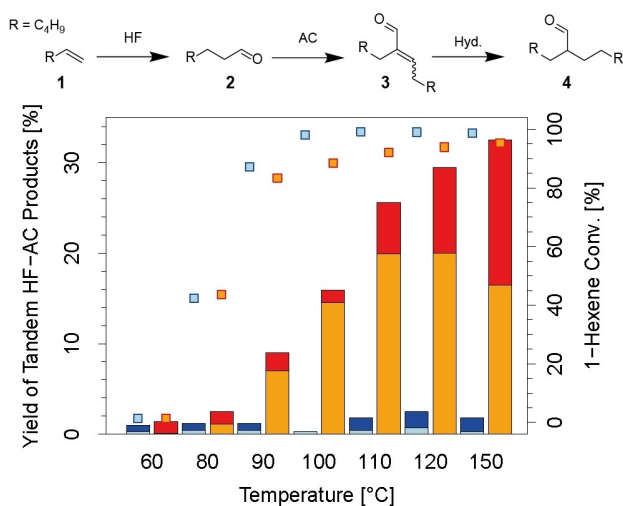
Chemistry–A European Journal

Research Article
doi.org/10.1002/chem.202300939

Chemistry Europe
European Chemical
Societies Publishing

Figure 4. Tandem HF-AC products **3** and **4** from 1-hexene at 80 bar syngas pressure (CO: H₂ = 1) as a function of temperature. Products of the homogeneous reaction (Co₂(CO)₈ (4.0 mg, 12 μmol) in 1-hexene (0.5 mL, 4.0 mmol)) are plotted in shades of blue, **3** (light blue), **4** (dark blue), whereas those yielded in the Zn-MOF-74-modified reaction (Co₂(CO)₈ (4.0 mg, 12 μmol), Zn-MOF-74 (20 mg, 43 μmol) in 1-hexene (0.5 mL, 4.0 mmol)) are depicted in orange (**3**) and red (**4**). The 1-hexene conversion of the corresponding reactions are plotted in the same colors. In this plot, **3** includes the AC products yielded from the aldol addition of two molecules of 1-heptanal and that of 2-methylhexanal with 1-heptanal.

highlight the pivotal role of Zn-MOF-74 in the tandem HF-AC reaction. For comparison, the zinc-based MOF ZIF-8[24] was tested in tandem HF-AC in the presence of Co₂(CO)₈ at 80 bar and 120 °C yielding **3** and **4** in 9.1% and 5.4%, respectively. Under the same conditions, Co-MOF-74 and Co₂(CO)₈ produced **3** in 0.2% and **4** in 4.3%. Co-MOF-74 in the absence of the homogeneous catalyst led to traces of **3** and **4** (Figure S10). These results emphasize the roles of zinc and the OMS as well as the necessity of the Co catalyst to yield efficient tandem HF-AC systems. Furthermore, they suggest that the basicity of the phenolate group has little influence on the AC activity since the less basic[25] Zn-MOF-74 displays superior performance over Co-MOF-74.

We characterized Zn-MOF-74 before and after the reaction at 110 °C by powder X-ray diffraction (PXRD) and nitrogen adsorption analyzed by the Brunauer-Emmett-Teller (BET) model. The PXRD pattern after the reaction was identical to that of pristine Zn-MOF-74 (Figure S2), demonstrating the structural integrity of the framework. The BET surface area decreased significantly from 1100 m²/g to 26 m²/g (Figure S6), suggesting the presence of residual molecules in the pores as reported elsewhere.[7a,d]

In order to gain a deeper insight into the role of the MOF in the tandem HF-AC, we performed density functional theory (DFT) calculations (see Supporting Information). The interaction energy between the product of the HF reaction (heptanal) and the free coordination site in Zn-MOF-74 was −101 kJ/mol. The structure of heptanal adsorbed within the pores of the MOF showed a longer carbonyl bond of 1.222 Å compared to the free aldehyde (1.209 Å). The net atomic charges were calculated

according to DDEC6 atomic population analysis,[26] showing that the charge of the carbonyl carbon atom increased from +0.414 in the free aldehyde to +0.461 in the adsorbed aldehyde, highlighting its enhanced electrophilic character. The aldehyde probably acts as a better electrophile when adsorbed within the MOF, thereby facilitating the reaction. Figure 5 illustrates the optimized structure of adsorbed heptanal (**2**@Zn-MOF-74).

The elongation of the carbonyl bond within Zn-MOF-74 was confirmed by Fourier-transform infrared spectroscopy (FTIR), which showed a reduction of the C=O stretch wavenumber from 1724 cm⁻¹ in the free aldehyde to 1698 cm⁻¹ in heptanal adsorbed within the MOF (Figure S11). Combined with the DFT calculations, the FTIR results imply that Zn-MOF-74 activates the aldehyde through adsorption. The interaction of Zn-MOF-74 and the Co catalyst was investigated by X-ray photoelectron spectroscopy (XPS). Zn 3p and O 1s core-levels of Zn-MOF-74, acquired before and after the reaction, yielded comparable photoemission spectra (Figure S13). The position and shape of the Zn 3p peaks (Zn 3p₃/₂ centered at 88.9 eV, spin orbit splitting of 2.1 eV) are in agreement with other literature reports of Zn(II) in MOFs,[27] confirming the expected oxidation state of zinc. The Co 2p spectrum of the sample after reaction is in fair agreement with previous literature on Co in MOF-74.[28] The main peak (2p₃/₂), centered at around 783.6 eV, together with its satellite at 787.9 eV indicate the presence of Co(II). This suggests that the MOF structure does not undergo relevant changes during the reaction, and identifies 2+ oxidation states for zinc and cobalt. The MOF was further characterized by in situ transmission IR spectroscopy. Spectra of activated Zn-MOF-74 with adsorbed deuterated acetonitrile (d3-ACN) show the extent of the MOF's Lewis acidity (Figure S3). The interaction of the OMS with the nitrile group leads to a blueshift of the C≡N stretch vibration to 2279 cm⁻¹ compared to liquid d3-ACN at 2263 cm⁻¹.[29] Figure S3 indicates the presence of a low amount of defects, as demonstrated by the lack of stronger blueshifted peaks[29d] and a relatively mild Lewis acidity, based on the shift of 16 cm⁻¹. The continuous redshift of the main nitrile band upon adsorption was associated to its coverage-dependent behavior. The redshifted peak at 2236 cm⁻¹ was
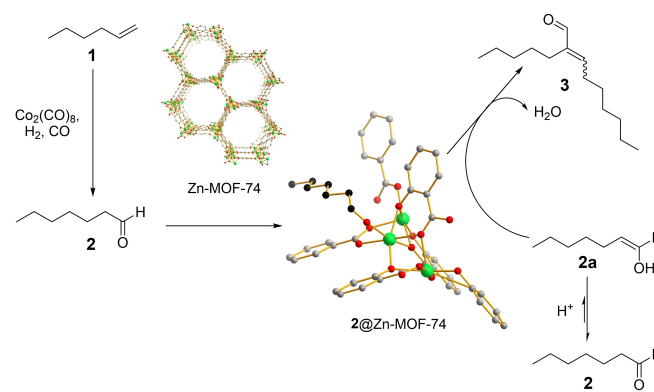

Figure 5. Proposed reaction mechanism of the adsorption-driven tandem HF-AC. Linear products only are shown for the sake of clarity. Color code: Zn-MOF-74 carbon (grey), aldehyde carbon (black), oxygen (red), zinc (green). Hydrogen is omitted for the sake of clarity.

assigned to the interaction of d3-ACN with the basic phenolate groups.[25,30] The interaction energies of the cobalt hydroformylation intermediates[31] with Zn-MOF-74 are summarized in Table S6. The acyl cobalt intermediate (Figure S15, **6**) features the strongest interaction energy with −127 kJ/mol. The Co−H bond lengths in the free hydride complex (Figure S15, **5**) and the bond length coordinated to Zn-MOF-74 are the same (1.488 Å), indicating that the MOF has little, if any, influence on the structure of cobalt tetracarbonyl hydride, the most likely Brønsted active site for the AC.[32]

Based on these results, we propose a preliminary reaction mechanism for the adsorption-driven tandem HF-AC promoted by MOF-74.[33] The data in Figure 2 show that Zn-MOF-74 alone is insufficient to efficiently promote the AC; we propose a cooperative mechanism involving the cobalt catalyst and the MOF. The precatalyst, $Co_2(CO)_8$, undergoes hydrogenolysis under the applied syngas conditions to form $HCo(CO)_4$,[34] which is a strong acid.[32] In a first step, the cobalt catalyst promotes the hydroformylation of **1** to the corresponding aldehydes. HF product **2** is then adsorbed by Lewis acidic sites in Zn-MOF-74, as observed by FTIR and simulated by DFT, thereby enhancing the electrophilic character of the carbonyl carbon atom (**2**@Zn-MOF-74). The Brønsted acid $HCo(CO)_4$ catalyzes the enolization of **2** to yield **2a**, which reacts with the adsorbed heptanal to form **3** upon release of water, typical for acid-catalyzed AC.[8a,33,35] A competition experiment where Zn-MOF-74 was treated at 120°C with both heptanal and water showed a shoulder at 1698 cm^{-1} in the FTIR spectrum of the recovered MOF. This band coincides with that of heptanal adsorbed to activated Zn-MOF-74, demonstrating that heptanal still adsorbs to the zinc OMS in the MOF even in the presence of water (Figure S12). The interaction energy of heptanal with zinc is −101 kJ/mol, higher than the adsorption energy of water (−60 to −65 kJ/mol), further confirming the experimental result.[36]

Conclusion

We report a catalytic system for the tandem HF-AC allowing the one-pot synthesis of α, β-unsaturated aldehydes from olefins and syngas working with a cobalt hydroformylation catalyst and Zn-MOF-74. The yield of AC products was enhanced up to 17-fold upon the addition of Zn-MOF-74 under very mild conditions of temperature and pressure. Catalytic experiments showed that both the cobalt catalyst and the MOF are essential to maximize the AC yield. FTIR and DFT calculations showed that the Zn sites within Zn-MOF-74 adsorb the aldehyde produced in the HF reaction, thus increasing the electrophilic character of the carbonyl carbon atom. The cobalt complex and the MOF components work cooperatively, where adsorption of the aldehyde plays a central role in enhancing the yield of the AC products.

Experimental Section

Zn-MOF-74: 2,5-Dihydroxyterephthalic acid (1.80 g, 9.08 mmol, 1.0 eq) and $Zn(acac)_2 \cdot H_2O$ (5.20 g, 18.5 mmol, 2.0 eq) were dissolved in a mixture of DMF (176 mL) and water (9 mL). This solution was split between three 100 mL EasyPrep vessels and placed in a microwave reactor (from rt to 130°C in 20 min, reaction at 130°C for 1 h) to give a yellow suspension. The solid was filtered off by a membrane filter and washed with dimethylformamide (DMF, 3× 100 mL, first time overnight), water (3×100 mL), EtOH (3×100 mL), and *tert*-butyl methyl ether (TBME, 3×100 mL). After that, the MOF was dried in a vacuum oven overnight at 60°C. Activation at 250°C in vacuum yielded Zn-MOF-74 (2.01 g, 68%) as a yellow solid. The PXRD pattern (Figure S2) is comparable to the reference pattern.[37] The BET surface area (Figure S6) was calculated as 1100 m^2/g, in good agreement with the literature.[38]

Tandem HF-AC: Important safety statement: CO is a toxic gas, and all manipulations should be carried out using a personal CO sensor in addition to a lab CO sensor. Zn-MOF-74 (20 mg, 43 μmol) was weighed into a 2 mL crimp vial and activated in vacuum at 150°C for 20 to 24 h in a round-bottom flask equipped with a glass valve. This leads to a weight loss of approximately 30%, which we considered for the calculation of the molar amount. The crimp vials were introduced to a glovebox, where a solution of $Co_2(CO)_8$ of the indicated concentration (3.2 mg/ml, 9.4 μmol/ml or 8.0 mg/ml, 24 μmol/ml) in 1-hexene (8.0 mmol/ml) was prepared. This solution (0.5 mL) was added to the crimp vials before they were sealed with new septa. The crimp vials were placed in an autoclave, which was then flushed with argon. While continuing flushing, the autoclave was opened, and the septa were pierced with a needle. The autoclave was closed, and flushing continued for 1 min. The autoclave was then pressurized to the indicated pressure with syngas (CO: H$_2$ = 1), and the system heated to the required temperature leading to a significant pressure increase. The reaction was allowed to take place for 16 h before the autoclave was cooled below a temperature of 30°C. The pressure was released slowly, and the autoclave flushed with argon before opening. Homogeneous reactions were performed equivalently without the addition of Zn-MOF-74. The content of the crimp vials was transferred into 5 mL volumetric flasks and filled with tetrahydrofuran (THF). Zn-MOF-74 was extracted for 30 min before 200 μL of the supernatant were diluted with 800 μL of the external standard (p-cymene 0.048 M in THF). This solution was analyzed by GC-FID and, upon appropriate dilution, by GC-MS.

Supporting Information

Additional experimental details, characterization results, and procedures are available in the Supporting Information.[37,39]

Acknowledgements

Conflict of Interests

The authors declare no conflict of interest.

Data Availability Statement

The data that support the findings of this study are available from the corresponding author upon reasonable request.

[1] H. Furukawa, K. E. Cordova, M. O'Keeffe, O. M. Yaghi, *Science* **2013**, *341*, 1230444.

[2] a) O. M. Yaghi, M. O'Keeffe, N. W. Ockwig, H. K. Chae, M. Eddaoudi, J. Kim, *Nature* **2003**, *423*, 705–714; b) S. Kitagawa, R. Kitaura, S.-i. Noro, *Angew. Chem. Int. Ed.* **2004**, *43*, 2334–2375.

[3] a) J. Lee, O. K. Farha, J. Roberts, K. A. Scheidt, S. T. Nguyen, J. T. Hupp, *Chem. Soc. Rev.* **2009**, *38*, 1450–1459; b) H. Jiang, W. Zhang, X. Kang, Z. Cao, X. Chen, Y. Liu, Y. Cui, *J. Am. Chem. Soc.* **2020**, *142*, 9642–9652; c) W. Zhang, W. Shi, W. Ji, H. Wu, Z. Gu, P. Wang, X. Li, P. Qin, J. Zhang, Y. Fan, T. Wu, Y. Fu, W. Zhang, F. Huo, *ACS Catal.* **2020**, *10*, 5805–5813; d) Y. Benseghir, A. Lemarchand, M. Duguet, P. Mialane, M. Gomez-Mingot, C. Roch-Marchal, T. Pino, M.-H. Ha-Thi, M. Haouas, M. Fontecave, A. Dolbecq, C. Sassoye, C. Mellot-Draznieks, *J. Am. Chem. Soc.* **2020**, *142*, 9428–9438.

[4] a) M. P. Suh, H. J. Park, T. K. Prasad, D.-W. Lim, *Chem. Rev.* **2012**, *112*, 782–835; b) A. Ahmed, S. Seth, J. Purewal, A. G. Wong-Foy, M. Veenstra, A. J. Matzger, D. J. Siegel, *Nat. Commun.* **2019**, *10*, 1568; c) W. L. Queen, M. R. Hudson, E. D. Bloch, J. A. Mason, M. I. Gonzalez, J. S. Lee, D. Gygi, J. D. Howe, K. Lee, T. A. Darwish, M. James, V. K. Peterson, S. J. Teat, B. Smit, J. B. Neaton, J. R. Long, C. M. Brown, *Chem. Sci.* **2014**, *5*, 4569–4581; d) J. A. Mason, M. Veenstra, J. R. Long, *Chem. Sci.* **2014**, *5*, 32–51.

[5] a) J.-R. Li, R. J. Kuppler, H.-C. Zhou, *Chem. Soc. Rev.* **2009**, *38*, 1477–1504; b) J. S. Yeon, W. R. Lee, N. W. Kim, H. Jo, H. Lee, J. H. Song, K. S. Lim, D. W. Kang, J. G. Seo, D. Moon, B. Wiers, C. S. Hong, *J. Mater. Chem. A* **2015**, *3*, 19177–19185; c) A. M. Fracaroli, H. Furukawa, M. Suzuki, M. Dodd, S. Okajima, F. Gandara, J. A. Reimer, O. M. Yaghi, *J. Am. Chem. Soc.* **2014**, *136*, 8863–8866; d) S. J. Geier, J. A. Mason, E. D. Bloch, W. L. Queen, M. R. Hudson, C. M. Brown, J. R. Long, *Chem. Sci.* **2013**, *4*, 2054–2061 ; e) E. D. Bloch, W. L. Queen, R. Krishna, J. M. Zadrozny, C. M. Brown, J. R. Long, *Science* **2012**, *335*, 1606–1610.

[6] R. Franke, D. Selent, A. Börner, *Chem. Rev.* **2012**, *112*, 5675–5732.

[7] a) G. Bauer, D. Ongari, D. Tiana, P. Gäumann, T. Rohrbach, G. Pareras, M. Tarik, B. Smit, M. Ranocchiari, *Nat. Commun.* **2020**, *11*, 1059; b) C. Hou, G. Zhao, Y. Ji, Z. Niu, D. Wang, Y. Li, *Nano Res.* **2014**, *7*, 1364–1369; c) S. Sartipi, M. J. Valero Romero, E. Rozhko, Z. Que, H. A. Stil, J. de With, F. Kapteijn, J. Gascon, *ChemCatChem* **2015**, *7*, 3243–3247; d) P. Tang, S. Paganelli, F. Carraro, M. Blanco, R. Ricco, C. Marega, D. Badocco, P. Pastore, C. J. Doonan, S. Agnoli, *ACS Appl. Mater. Interfaces* **2020**, *12*, 54798–54805; e) T. Van Vu, H. Kosslick, A. Schulz, J. Harloff, E. Paetzold, H. Lund, U. Kragl, M. Schneider, G. Fulda, *Microporous Mesoporous Mater.* **2012**, *154*, 100–106; f) T. Van Vu, H. Kosslick, A. Schulz, J. Harloff, E. Paetzold, M. Schneider, J. Radnik, N. Steinfeldt, G. Fulda, U. Kragl, *Appl. Catal. A* **2013**, *468*, 410–417; g) T. Van Vu, H. Kosslick, A. Schulz, J. Harloff, E. Paetzold, J. Radnik, U. Kragl, G. Fulda, C. Janiak, N. D. Tuyen, *Microporous Mesoporous Mater.* **2013**, *177*, 135–142.

[8] a) J. Clayden, N. Greeves, S. Warren, *Organic Chemistry*, 2 ed., Oxford University Press, Oxford, **2012**; b) L. Zhu, X. Q. Liu, H. L. Jiang, L. B. Sun, *Chem. Rev.* **2017**, *117*, 8129–8176.

[9] V. Nair, R. S. Menon, A. T. Biju, C. R. Sinu, R. R. Paul, A. Jose, V. Sreekumar, *Chem. Soc. Rev.* **2011**, *40*, 5336–5346.

[10] a) A. Schönweiz, J. Debuschewitz, S. Walter, R. Wölfel, H. Hahn, K. M. Dyballa, R. Franke, M. Haumann, P. Wasserscheid, *ChemCatChem* **2013**, *5*, 2955–2963; b) P. W. N. M. v. Leeuwen, C. Claver, *Rhodium Catalyzed Hydroformylation*, Kluwer Academic Publishers, New York, **2002**; c) Y. Sun, J. Harloff, H. Kosslick, A. Schulz, C. Fischer, S. Bartling, M. Frank, A. Springer, *J. Mol. Catal.* **2022**, *517*, 112005.

[11] E. B. M. Doesburg, J. W. Geus, F. Kapteijn, G. B. Marin, J. A. Moulijn, J. W. Niemantsverdriet, B. E. Nieuwenhuys, V. Ponec, J. J. F. Scholten, R. A. Sheldon, A. Tarfaoui, H. v. Bekkum, J. H. C. v. Hooff, G. v. Koten, P. W. N. M. v. Leeuwen, R. A. v. Santen, J. A. R. v. Veen, in *Stud. Surf. Sci. Catal., Vol. 79* (Eds.: J. A. Moulijn, P. W. N. M. van Leeuwen, R. A. van Santen), Elsevier, Amsterdam, **1993**, pp. 199–248.

[12] Ceresana, "Marktsudie Weichmacher - Welt", can be found under: http://www.ceresana.com/de/marktstudien/chemikalien/weichmacher/, **2021**.

[13] G. Kessen, B. Cornils, J. Hibel, H. Bach, W. Gick (Hoechst AG), EP0216151B1, **1991**.

[14] J. J. J. McKetta, W. Cunningham, in *Encyclopedia of Chemical Processing and Design, Vol. 5*, Marcel Dekker, New York, **1977**.

[15] N. L. Cull, C. L. Aldridge, J. K. Mertzweiller (ExxonMobil Research and Engineering Co), US2845465 A, **1958**.

[16] C. R. Greene (Shell Oil Co), US3278612 A, **1966**.

[17] X. Fang, R. Jackstell, R. Franke, M. Beller, *Chem. Eur. J.* **2014**, *20*, 13210–13216.

[18] Y.-Q. Li, Q. Zhou, D.-L. Wang, P. Wang, Y. Lu, Y. Liu, *J. Mol. Catal.* **2017**, *439*, 25–30.

[19] a) V. K. Srivastava, S. K. Sharma, R. S. Shukla, R. V. Jasra, *Catal. Commun.* **2006**, *7*, 879–884; b) S. K. Sharma, P. A. Parikh, R. V. Jasra, *J. Mol. Catal. A* **2009**, *301*, 31–38.

[20] M. Strohmann, J. T. Vossen, A. J. Vorholt, W. Leitner, *Green Chem.* **2020**, *22*, 8444–8451.

[21] L. Kollár, P. Pongrácz, *J. Organomet. Chem.* **2018**, *866*, 184–188.

[22] a) R. V. Gholap, O. M. Kut, J. R. Bourne, *Ind. Eng. Chem. Res.* **1992**, *31*, 1597–1601; b) M. Hidai, A. Fukuoka, Y. Koyasu, Y. Uchida, *J. Mol. Catal.* **1986**, *35*, 29–37; c) A. M. Kluwer, M. J. Krafft, I. Hartenbach, B. de Bruin, W. Kaim, *Top. Catal.* **2016**, *59*, 1787–1792.

[23] a) O. Roelen (Chemische Verwertungsgesellschaft Oberhausen), DE849548 C, **1952**; b) B. Cornils, J. Hibbel, G. Kessen, W. Konkol, B. Lieder, E. Wiebus, H. Kalbfell, H. Bach (Ruhrchemie AG), EP0111257 A1, **1984**; c) W. Reppe, H. Eilbracht (Chemische Verwertungsgesellschaft Oberhausem), DE891688 C, **1953**.

[24] a) R. Banerjee, A. Phan, B. Wang, C. Knobler, H. Furukawa, M. O'Keeffe, O. M. Yaghi, *Science* **2008**, *319*, 939–943; b) K. S. Park, Z. Ni, A. P. Côté, J. Y. Choi, R. Huang, F. J. Uribe-Romo, H. K. Chae, M. O'Keeffe, O. M. Yaghi, *Proc. Nat. Acad. Sci.* **2006**, *103*, 10186–10191.

[25] P. Valvekens, M. Vandichel, M. Waroquier, V. Van Speybroeck, D. De Vos, *J. Catal.* **2014**, *317*, 1–10.

[26] T. A. Manz, N. G. Limas, *RSC Adv.* **2016**, *6*, 47771–47801.

[27] a) D. K. Yadav, R. Gupta, V. Ganesan, P. K. Sonkar, M. Yadav, *ChemElectroChem* **2018**, *5*, 2612–2619; b) F. Gu, H. Chen, D. Han, Z. Wang, *RSC Adv.* **2016**, *6*, 29727–29733.

[28] F. Shi, Z. Wang, K. Zhu, X. Zhu, W. Yang, *Electrochim. Acta* **2022**, *416*.

[29] a) V. Guillerm, F. Ragon, M. Dan-Hardi, T. Devic, M. Vishnuvarthan, B. Campo, A. Vimont, G. Clet, Q. Yang, G. Maurin, G. Ferey, A. Vittadini, S. Gross, C. Serre, *Angew. Chem. Int. Ed.* **2012**, *51*, 9267–9271; b) Z. Hu, D. Zhao, *CrystEngComm* **2017**, *19*, 4066–4081; c) C. Palomino Cabello, G. Gomez-Pozuelo, M. Opanasenko, P. Nachtigall, J. Cejka, *ChemPlusChem* **2016**, *81*, 828–835; d) C. Volkringer, H. Leclerc, J.-C. Lavalley, T. Loiseau, G. Férey, M. Daturi, A. Vimont, *J. Phys. Chem. C* **2012**, *116*, 5710–5719.

[30] W. R. Fawcett, G. Liu, T. E. Kessler, *J. Phys. Chem.* **1993**, *97*, 9289–9298.

[31] a) R. F. Heck, D. S. Breslow, *J. Am. Chem. Soc.* **1961**, *83*, 4023–4027; b) S. Maeda, K. Morokuma, *J. Chem. Theory Comput.* **2012**, *8*, 380–385.

[32] a) K. T. Quisenberry, T. P. Hanusa, in *Encyclopedia of Inorganic and Bioinorganic Chemistry* (Ed.: R. A. Scott), Wiley, **2011**; b) F. Hebrard, P. Kalck, *Chem. Rev.* **2009**, *109*, 4272–4282.

[33] A. T. Nielsen, W. J. Houlihan, in *Organic Reactions*, **2011**, pp. 1–438.

[34] J. W. Rathke, R. J. Klingler, T. R. Krause, *Organometallics* **1992**, *11*, 585–588.

[35] L. M. Baigrie, R. A. Cox, H. Slebocka-Tilk, M. Tencer, T. T. Tidwell, *J. Am. Chem. Soc.* **1985**, *107*, 3640–3645.

[36] a) Y. Li, X. Wang, D. Xu, J. D. Chung, M. Kaviany, B. Huang, *J. Phys. Chem. C* **2015**, *119*, 13021–13031; b) C. Romero-Muñiz, J. M. Gavira-Vallejo, P. J. Merkling, S. Calero, *ACS Appl. Mater. Interfaces* **2020**, *12*, 54980–54990; c) B. Vlaisavljevich, J. Huck, Z. Hulvey, K. Lee, J. A. Mason, J. B. Neaton, J. R. Long, C. M. Brown, D. Alfe, A. Michaelides, B. Smit, *J. Phys. Chem. A* **2017**, *121*, 4139–4151.

[37] W. Wong-Ng, J. A. Kaduk, H. Wu, M. Suchomel, *Powder Diffr.* **2012**, *27*, 256–262.

[38] I. Choi, Y. E. Jung, S. J. Yoo, J. Y. Kim, H.-J. Kim, C. Y. Lee, J. H. Jang, *J. Electrochem. Sci. Technol.* **2017**, *8*, 61–68.

Chemistry–A European Journal

Research Article
doi.org/10.1002/chem.202300939

Chemistry
Europe
European Chemical
Societies Publishing

[39] a) F. Orlando, A. Waldner, T. Bartels-Rausch, M. Birrer, S. Kato, M.-T. Lee, C. Proff, T. Huthwelker, A. Kleibert, J. van Bokhoven, M. Ammann, *Top. Catal.* **2016**, *59*, 591–604; b) K. Roy, L. Artiglia, J. A. van Bokhoven, *ChemCatChem* **2018**, *10*, 666–682; c) S.-J. Lee, K. C. Kim, T.-U. Yoon, M.-B. Kim, Y.-S. Bae, *Microporous Mesoporous Mater.* **2016**, *236*, 284–291; d) W. Morris, C. J. Stevens, R. E. Taylor, C. Dybowski, O. M. Yaghi, M. A. Garcia-Garibay, *J. Phys. Chem. C* **2012**, *116*, 13307–13312; e) Y.-R. Lee, M.-S. Jang, H.-Y. Cho, H.-J. Kwon, S. Kim, W.-S. Ahn, *Chem. Eng. J.* **2015**, *271*, 276–280; f) T. Arii, A. Kishi, *J. Therm. Anal. Calorim.* **2006**, *83*, 253–260; g) K. Cebular, B. D. Bozic, S. Stavber, *Molecules* **2019**, *24*, 2608; h) G. Damilano, K. Binnemans, W. Dehaen, *Org. Biomol. Chem.* **2019**, *17*, 9778–9791; i) M. J. Frisch, G. W. Trucks, H. B. Schlegel, G. E. Scuseria, M. A. Robb, J. R. Cheeseman, G. Scalmani, V. Barone, G. A. Petersson, H. Nakatsuji, X. Li, M. Caricato, A. V. Marenich, J. Bloino, B. G. Janesko, R. Gomperts, B. Mennucci, H. P. Hratchian, J. V. Ortiz, A. F. Izmaylov, J. L. Sonnenberg, Williams, F. Ding, F. Lipparini, F. Egidi, J. Goings, B. Peng, A. Petrone, T. Henderson, D. Ranasinghe, V. G. Zakrzewski, J. Gao, N. Rega, G. Zheng, W. Liang, M. Hada, M. Ehara, K. Toyota, R. Fukuda, J. Hasegawa, M. Ishida, T. Nakajima, Y. Honda, O. Kitao, H. Nakai, T. Vreven, K. Throssell, J. A. Montgomery Jr., J. E. Peralta, F. Ogliaro, M. J. Bearpark, J. J. Heyd, E. N. Brothers, K. N. Kudin, V. N. Staroverov, T. A. Keith, R. Kobayashi, J. Normand, K. Raghavachari, A. P. Rendell, J. C. Burant, S. S. Iyengar, J. Tomasi, M. Cossi, J. M. Millam, M. Klene, C. Adamo, R. Cammi, J. W. Ochterski, R. L. Martin, K. Morokuma, O. Farkas, J. B. Foresman, D. J. Fox, Gaussian 16 Rev. C.01, **2016**, ; j) H. S. Yu, X. He, D. G. Truhlar, *J. Chem. Theory Comput.* **2016**, *12*, 1280–1293; k) F. Weigend, *Phys. Chem. Chem. Phys.* **2006**, *8*, 1057–1065; l) P. Verma, X. Xu, D. G. Truhlar, *J. Phys. Chem. C* **2013**, *117*, 12648–12660; m) J. Tomasi, B. Mennucci, R. Cammi, *Chem. Rev.* **2005**, *105*, 2999–3094.